A previously ignored scene-selective site is the key to encoding ego-motion in natural environments

Authors: Bryan Kennedy[1], Sarala N. Malladi[1], Shahin Nasr[1-2]

1) Athinoula A. Martinos Center for Biomedical Imaging, Massachusetts General Hospital, Charlestown, MA, United States

2) Department of Radiology, Harvard Medical School, Boston, MA, United States

Corresponding author: Dr. Shahin Nasr, Ph. D.

Address: Bldg. 149, 13th Street, Charlestown, MA 02176, USA

Email address: shahin.nasr@mgh.harvard.edu

Highlights

- There is a scene-selective site within the human posterior intraparietal gyrus.
- This site, named PIGS, was consistently detectable across subjects.
- In contrast to the other scene-selective areas, PIGS activity was influenced by ego-motion through scenes.

Abstract

The current models of scene processing in human brain are based on three scene-selective areas: the parahippocampal place area (PPA), the restrosplenial cortex (RSC) and the transverse occipital sulcus (TOS). In this study, we challenged this simplistic model by showing that other scene-selective sites can also be detected across the visual cortex, including one site within the posterior intraparietal gyrus. Despite the smaller size of this site compared to the other scene-selective areas, the posterior intraparietal gyrus scene-selective (PIGS) site was detected consistently in a large pool of subjects (*n*=45). The reproducibility of this finding was tested based on multiple criteria, including comparing the results across sessions, utilizing different scanners (3T vs. 7T) and stimulus sets. Furthermore, by showing that this site (but not PPA, RSC and/or TOS) is significantly sensitive to the interaction between scene presentation and ego-motion, we distinguished the PIGS role in scene perception from the other scene-selective areas. These results highlight the importance of including finer scale scene-selective sites, beyond PPA, RSC and TOS, in models of scene processing – a crucial step toward a more comprehensive understanding of how scenes are encoded under dynamic conditions.

Keywords: Scene perception, ego-motion, intraparietal gyrus, fine-scale functional organization

1. Introduction

In human and non-human primates (NHPs), fMRI has been used for many decades to localize the cortical regions that are preferentially involved in scene perception (Epstein and Kanwisher, 1998; Nasr *et al.*, 2011; Rajimehr *et al.*, 2009; Tsao *et al.*, 2008). For a variety of reasons, including the relatively low contrast to noise ratio of fMRI signal in lower magnetic fields, early studies struggled with the reliability of their findings. Consequently, these studies focused mainly on larger activity sites that were more easily reproducible across sessions and individuals, ignoring smaller sites that were not detectable in all subjects and/or were not reproducible across scan sessions. This left us with relatively simplistic models of neuronal processing solely based on larger visual areas.

Specifically, the initial studies of scene perception suggested that there are three scene-selective areas within the visual cortex of human and NHPs (Nasr *et al.*, 2011). These areas were originally named parahippocampal place area (PPA) (Epstein and Kanwisher, 1998; Levy *et al.*, 2004), retrosplenial cortex (RSC) (Maguire, 2001; Park and Chun, 2009) and transverse occipital sulcus TOS/OPA (Dilks *et al.*, 2013; Grill-Spector, 2003), after the adjacent anatomical landmarks. The idea that scene-selective areas are limited to these three regions is mostly based on group-averaged activity maps, generated after applying large surface/volume-based smoothing to the data from individual subjects. As demonstrated in Figure 1A, outcomes of this approach, especially in higher threshold levels, is usually limited to the three aforementioned sites.

However, on the single subject level, multiple smaller scene-selective sites could be detected outside these scene-selective areas, especially when drastic spatial smoothing is avoided (Figure 1B). This phenomenon is highlighted in a recent neuroimaging study in NHPs (Li *et al.*, 2022) in which authors took advantage of high-resolution neuroimaging techniques based on using implanted head coils. Their findings suggested that scene-selective areas are likely not limited to three hubs and that other, smaller, scene-selective areas could be also detected across the brain. Still, the reliability in detection of these smaller sites, their spatial consistency across large populations and more importantly, their specific role in scene perception that distinguishes them from the other scene-selective areas, remain unclear.

In this study, we used conventional (based on using 3T scanner) and high-resolution (based on using 7T scanner) fMRI to localize and study the fine-scale scene-selective sites that were detected outside PPA, RSC and TOS. By focusing our efforts on the intraparietal region, we

found an additional scene-selective area within the posterior intraparietal gyrus, adjacent to the motion-selective area V6 (Dechent and Frahm, 2003; Pitzalis *et al.*, 2009). The posterior intraparietal gyrus scene-selective (PIGS) site was detected consistently across individual subjects and populations. This site was localized reliably across scan sessions and showed sensitivity to ego-motion within scenes, a phenomenon not detectable in other scene-selective areas.

2. Methods

2.1. Participants

Forty-five human subjects (25 females), aged 22-40 years, participated in this study. All subjects had normal or corrected-to-normal vision and radiologically normal brains, without any history of neuropsychological disorder. All experimental procedures conformed to NIH guidelines and were approved by Massachusetts General Hospital protocols. Written informed consent was obtained from all subjects before the experiments.

2.2. General procedure:

This study consists of 6 experiments during which we used fMRI to localize and to study the evoked scene-selective responses. During these experiments, stimuli were presented via a projector (1024 × 768 pixel resolution, 60 Hz refresh rate) onto a rear-projection screen. Subjects viewed the stimuli through a mirror mounted on the receive coil array. Details of these stimuli are described in the following sections.

During all experiments, to make sure that subjects were attending to the screen, they were instructed to report color changes (red to blue and vice versa) for a centrally presented fixation object (0.1˚ × 0.1˚) by pressing a key on the keypad. Subject detection accuracy remained above 75% and they showed no significant difference in color change detection performance across experimental conditions (p>0.10). MATLAB (MathWorks; Natick, MA, USA) and the Psychophysics Toolbox (Brainard, 1997; Pelli, 1997) were used to control stimulus presentation.

2.2.1. Experiment 1 – Localization of scene-selective areas: In fourteen subjects (6 females), we localized scene-selective areas PPA, RSC and TOS/OPA by measuring their evoked brain activity, using a 3T fMRI scanner, as they were presented with 8 colorful images of real-world scenes vs. faces. Scene and face images subtended 20˚ × 26˚ of visual field and

were presented in different blocks (16 s per block and 1 s per image). Each subject participated in 4 runs and each run consisted of 10 blocks plus 32 s of blank presentation at the beginning and at the end of each block. In each run, the sequence of blocks and the sequence of images within them was randomized.

2.2.2. Experiment 2 – PIGS reproducibility across scan sessions (3T vs. 7T): To localize PIGS with higher spatial resolution and to enhance signal/contrast to noise ratio (relative to Experiment 1), four subjects were randomly selected from those who participated in Experiment 1 and were scanned in a 7T scanner. These individuals were presented with 300 grayscale images of scenes and 48 grayscale images of faces (20˚ × 26˚). Scene images included pictures of indoor (100 images), manmade outdoor (100 images) and natural outdoor (100 images) scenes, selected from Southampton-York Natural Scenes (SYNS) dataset (Adams *et al.*, 2016). These images were different than those used in Experiment 1.

As in Experiment 1, face and scene images were presented across different blocks. Each block contained 24 stimuli (1 s per stimuli) with no blank presentation between the stimuli. The sequence of stimuli within the blocks was randomized. Each subject participated in 12 runs (11 blocks per run; 24 s per block; 1 s per stimulus), beginning and ending with an additional block (12 s) of uniform black presentation. In each run, the sequence of blocks and the sequence of images within them was randomized.

2.2.3. Experiment 3 – Localization of area V6: This experiment was designed to clarify the relative localization of PIGS vs. area V6 (Dechent and Frahm, 2003; Pitzalis *et al.*, 2009). All fourteen subjects who participated in Experiment 1 were examined again in a separate scan session using a 3T scanner. During this scan session, we localized area V6 by contrasting the response evoked by coherent radially-moving (optic flow) vs. randomly-moving dots (20˚ × 26˚), presented against a black background. The experiment was block-designed, and each block took 16 s, beginning and ending with an additional block of 16 s uniform black presentation. Other details of the experiment were similar to Experiment 1.

2.2.4. Experiment 4 – PIGS localization in a larger population: Considering the small size of PIGS, it was important to show this area could survive group-averaging over larger populations compared to Experiment 1. Accordingly, Experiment 4 localized this area in a large pool of subjects, consisted of thirty-one individuals (19 females) other than those who participated in

Experiment 1. The stimuli and procedure were identical to Experiment 1.

2.2.5. Experiment 5 – Response to an independent set of scenes, non-scene objects: Experiments 1-4 used the response evoked by scenes vs. faces to localize PIGS. Considering that "scenes vs. faces" contrast evoked the strongest response within the scene-selective areas, it remains unknown whether PIGS also showed a selective response to the "scenes vs. objects" contrast. Accordingly, Experiment 5 tested the response evoked by scene vs. non-scene objects (faces not included) in PIGS and the adjacent areas V6, TOS and RSC. Thirteen subjects (7 females) were randomly-selected from those who participated in Experiment 4 and scanned in a 3T scanner. They were presented with 22 grayscale images of scenes, and 88 grayscale images of everyday non-animated objects. All stimuli were presented within a circular aperture (diameter=20˚). Notably, scene images used in this experiment were different than those used in Experiments 1-4. Scene and object images were presented in different blocks according to their category (22 s per block and 1 s per image). Each subject participated in 12 runs and each run consisted of 9 blocks, plus 16 s of blank presentation at the beginning and the end of each block. As in other experiments, the sequence of blocks and the sequence of images within them was randomized.

2.2.6. Experiment 6 – Coherently vs. incoherently changing scenes: This experiment was designed to compare/differentiate PIGS role in scene perception from IPA/TOS, RSC and PPA. Twelve subjects, from the fourteen subjects who participated in Experiment 1, participated in this experiment. The excluded two subjects could not participate further in our tests for personal reasons. Subjects were scanned in a 3T scanner on a different day relative to Experiments 1-3. During this scan, they were presented with rapid coherently vs. incoherently changing grayscale scenes (100 ms per image), across different blocks (16 s per block).

Coherently changing scenes implied ego-motion (fast walking) along 3 different outdoor natural trails. Stimuli (20˚ × 26˚) were generated as one of the experimenters walked through the trails while carrying a camera mounted on his forehead and took pictures every 2 meters. Incoherently changing scenes consisted of the same images as the coherently changing blocks but with randomized order. For both coherently and incoherently changing scenes, images from different trails were presented across different blocks. In separate blocks, subjects were also presented with 80 grayscale face images (20˚ × 26˚) with the same timing (i.e. 100 ms per image; 16 s per block). Each subject participated in 6 runs and each run consisted of 9 blocks, plus 8 s of blank presentation at the beginning and the end of each block and 4 s of blank

presentation between blocks.

On different runs (within the same session), subjects were also presented with concentric rings, extending 20° × 26° (height × width) in the visual field, presented against a light gray background (40 cd/m^2). In half of the blocks (16 s per block), rings moved radially (centrifugally vs. centripetally; 4°/s) and the direction of motion changed every 4 s to reduce the impact of motion after-effects. In the other half of blocks, rings remained stationary during the whole block. Each subject participated in 2 runs and each run consisted of 8 blocks, plus 16 s of uniform gray presentation at the beginning and the end of each run. The sequence of moving and stationary blocks was pseudo-randomized across runs.

2.3. Imaging:

2.3.1. 3T scans: In Experiments 1 and 3-6, subjects were scanned in a horizontal 3T scanner (Tim Trio, Siemens Healthcare, Erlangen, Germany). Gradient echo EPI sequences were used for functional imaging during tasks. Functional data were acquired using single-shot gradient echo EPI with nominally 3.0 mm isotropic voxels (TR=2000 ms; TE=30 ms; flip angle=90°; Band Width (BW)=2298 Hz/pix; echo-spacing= 0.5 ms; no partial Fourier; 33 axial slices covering the entire brain; and no acceleration). During the first 3T scan (see the General Procedure), structural (anatomical) data were acquired for each subject using a 3D T1-weighted MPRAGE sequence (TR=2530 ms; TE=3.39 ms; TI=1100 ms; flip angle=7°; BW=200 Hz/pix; echo-spacing=8.2 ms; voxel size=1.0×1.0×1.33 mm).

2.3.2. 7T scans: In Experiment 2, subjects were scanned in a 7T Siemens whole-body scanner (Siemens Healthcare, Erlangen, Germany) equipped with SC72 body gradients (maximum gradient strength, 70 mT/m; maximum slew rate, 200 T/m/s) using a custom-built 32-channel helmet receive coil array and a birdcage volume transmit coil. Voxel dimensions were nominally 1.0 mm, isotropic. Single-shot gradient-echo EPI was used to acquire functional images with the following protocol parameter values: TR=3000 ms; TE=28 ms; flip angle=78°; BW=1184 Hz/pix; echo-spacing=1 ms; 7/8 phase partial Fourier; 44 oblique-coronal slices; and acceleration factor r=4 with GRAPPA reconstruction and FLEET-ACS data (Polimeni *et al.*, 2015) with 10° flip angle. The field of view included the occipital-parietal brain areas to cover PIGS, RSC and TOS (but not PPA).

2.4. Data Analysis:

2.4.1. Structural data analysis: For each subject, inflated and flattened cortical surfaces were reconstructed based on the high-resolution anatomical data (Dale *et al.*, 1999; Fischl *et al.*, 2002; Fischl *et al.*, 1999), during which the standard pial surface was generated as the gray matter border with the surrounding cerebrospinal fluid or CSF (i.e. GM-CSF interface). The white matter surface was also generated as the interface between white and gray matter (i.e. WM-GM interface). In addition, an extra surface was generated at 50% of the depth of the local gray matter (Dale *et al.*, 1999).

2.4.2. Individual-level functional data analysis: All functional data were rigidly aligned (6 df) relative to subject's own structural scan, using rigid Boundary-Based Registration (Greve and Fischl, 2009), and then were motion corrected. Data collected in the 3T (but not 7T) scanner was spatially smoothed using a 3D Gaussian kernel (2 mm FWHM). To preserve the spatial resolution, data collected within the 7T scanner was not spatially smoothed.

Subsequently, A standard hemodynamic model based on a gamma function was fit to the fMRI signal to estimate the amplitude of the BOLD response. For each individual subject, the average BOLD response maps were calculated for each condition (Friston *et al.*, 1999). Finally, voxel-wise statistical tests were conducted by computing contrasts based on a univariate general linear model.

The resultant significance maps based on 3T scans were sampled from the middle of cortical gray matter (defined for each subject based on their structural scan (see section 2.4.1)). For 7T scans, the resultant significance maps were sampled from deep cortical layers at the gray-white matter interface. This procedure reduces the spatial blurring caused by superficial veins (De Martino *et al.*, 2013; Koopmans *et al.*, 2010; Nasr *et al.*, 2016; Polimeni *et al.*, 2010). For presentation, the resultant maps were projected either onto the subject's reconstructed cortical surfaces or onto a common template (fsaverage; freesurfer (Fischl, 2012)).

2.4.3. Group-level functional data analysis: To generate group-averaged maps, functional maps were spatially normalized across subjects and then averaged using random-effects models and corrected for multiple comparisons (Friston *et al.*, 1999). Notably, for Figure 1A and to replicate our original finding (Nasr *et al.*, 2011), the group-average maps were generated using fixed-effects. The resultant significance maps were projected onto a common human brain template (fsaverage).

2.4.4. Region of interest (ROI) analysis: The main ROIs included area PIGS, the two adjacent scene-selective areas (RSC, TOS) and area V6. In Experiment 6, we also included area PPA in our analysis. These ROIs were localized in two different ways: (1) functionally for each subject based on their own evoked activity (section 2.4.4.1), and (2) probabilistically based on activity measured in a different group of subjects (section 2.4.4.2).

2.4.4.1. Functionally-localized ROIs: For those subjects who participated in Experiment 6, we localized scene-selective areas PIGS, TOS, RSC, and PPA based on their stronger response to scenes compared to faces at a threshold level of $p<10^{-2}$, using the method described in Experiment 1. For these individuals, we also localized area V6 based on the expected selective response in this region to coherent radially- vs. incoherently-moving random dots (see Section 2.2.3). In those subjects that PIGS and V6 showed partial overlap, the overlapping parts were excluded for the analysis.

2.4.4.2. Probabilistically-localized ROIs: For those subjects who participated in Experiments 4 and 5, we tested the consistency of PIGS locations across populations, using probabilistic labels for areas PIGS, TOS, RSC and V6. These labels were generated based on the results of Experiment 1 (for PIGS, TOS and RSC) and Experiment 3 (for V6). Specifically, we localized the ROIs separately for the individual subjects who participated in Experiments 1 and 3. Then the labels were overlaid on a common brain template (fsaverage). We computed the probability that each vortex within the cortical surface belonged to one of the ROIs. The labels for PIGS, TOS, RSC and V6 were generated based on those vertices that showed higher than 20% probability. This method assured us that our measurements were not biased by those subjects who showed stronger scene-selective responses. Moreover, by selecting a relatively low threshold (i.e. 20%), we avoided confining our ROIs to the center of activity sites.

2.4.5. Statistical tests: To test the effect of independent parameters, we applied paired t-tests and/or a repeated-measures ANOVA, with Greenhouse-Geisser correction whenever the sphericity assumption was violated.

2.5. Data sharing statement: All data, codes and stimuli are ready to be shared upon request.

3. Results

This study consists of six experiments. Experiment 1 focused on localizing the scene-selective site (PIGS) within the posterior intraparietal region. Experiment 2 showed consistency in the spatial location of PIGS across sessions. Experiment 3 examined PIGS location relative to V6, an area involved in motion coherency and optic flow encoding. Experiment 4 showed that, despite its small size, PIGS is detectable in group-averaged maps in large populations. Experiment 5 showed that scene and non-scene objects are differentiable from each other based on the evoked response evoked within PIGS. Finally, experiment 6 highlighted PIGS response to the interaction between the effects of scene and ego-motion presentation – a phenomenon that differentiated PIGS from the other scene-selective regions.

3.1. Experiment 1 – Small scene-selective sites are detectable within the posterior intraparietal gyrus

As mentioned above, scene-selective sites (other than PPA, TOS and RSC) are detectable across the brain, especially within the posterior intraparietal gyrus, when the level of spatial smoothing is relatively low (Figure 1B). To test the consistency in location of these scene-selective sites across individuals, fourteen subjects were presented with scene and face stimuli while we collected their fMRI activity. Considering the expected small size of the scene-selective sites within the intraparietal region, we used limited signal smoothing in our analysis (FWHM = 2 mm; see Methods) to increase the chance of detecting these sites.

Figure 2 shows the activity maps evoked by “scenes > faces” contrast in seven exemplar subjects. All activity maps were overlaid on a common brain template to highlight the consistency in location of scene-selective sites across individuals. In all tested individuals, besides areas RSC and TOS, we detected at least one scene-selective site within the posterior portion of the intraparietal gyrus, close to (but outside) the parieto-occipital sulcus (POS). Accordingly, we named this site the posterior interparietal gyrus scene-selective site or PIGS.

When measured at the same threshold levels ($p<0.05$), the size of PIGS was on average 73.86% ± 49.01% (mean ± S. D.) of RSC, 28.26% ± 15.67% of TOS, and 19.45% ± 8.43% of PPA. Considering PIGS location (close to the skull and head coil surface (Figure 1)), the relatively small size of PIGS could not be due to the lower signal/contrast to noise ratio in that region.

To better clarify the consistency of PIGS localization across subjects, we also generated group-averaged activity maps based on random-effects, and after correction for multiple comparisons. As demonstrated in Figure 3A, PIGS was also detectable in the group-averaged

activity maps, in almost the same location as in the individual subject maps. Overall, these results suggests that, despite the relatively small size of this scene-selective site, PIGS is consistently detectable across subjects in the same cortical location.

3.2. Experiment 2 – PIGS reproducibility across scan sessions

To test the reproducibility of our results, four subjects were selected randomly among those who participated in Experiment 1. These subjects were scanned again (on a different day), using a 7T (rather than a 3T) scanner, and a different set of scenes and faces (Figure 4A).

As demonstrated in Figure 4, despite using a different scanner and a different set of stimuli, PIGS was still detectable in the same location (Figure 4B-D). Specifically, in both scans, PIGS was localized within the posterior portion of the intraparietal gyrus and close to the posterior lip of parieto-occipital sulcus. Considering the higher contrast/signal to noise ratio of 7T (compared to 3T) scans, this result ruled out the possibility that PIGS is simply caused by nuisance artifacts in fMRI measurements.

3.3. Experiment 3 – Localization of areas PIGS vs. V6

Posterior intraparietal region also accommodates area V6 which is involved in motion coherency (optic-flow) encoding (Dechent and Frahm, 2003; Pitzalis *et al.*, 2009). More recent studies have suggested that scene stimuli evoke a strong response within V6 (Sulpizio *et al.*, 2020). To test whether PIGS overlaps with area V6, we localized this area in all subjects who participated in Experiment 1, based on using random vs. radially moving dots (see Methods).

Figure 4D shows the co-localization of V6 and PIGS in four individual subjects. Consistent with previous studies of V6 (Dechent and Frahm, 2003; Pitzalis *et al.*, 2015; Pitzalis *et al.*, 2009), this area was localized *within* the posterior portion of the POS without any overlap between its center and PIGS.

To test the relative localization of these two regions in group-levels, we generated probabilistic labels for PIGS and V6 (see Methods). As demonstrated in Figure 5, the probabilistic label for PIGS was localized within the intraparietal gyrus and outside the POS (Figure 5A), while V6 was located within the POS (Figure 5B). We also did not find any overlap between area V6 and areas RSC and TOS (Figure 5C). Thus, despite the low threshold level used to generate these labels (probability>20%), the areas PIGS and V6 appeared side-by-side (Figure 5D) without any overlapping between their centers.

3.4. Experiments 4 – PIGS localization in a larger population

Results of Experiments 1-3 suggests that PIGS could be located consistently across individual subjects, and that this area appears to be distinguishable from the adjacent area V6. However, considering the small size of this area, it appears necessary to test whether this area was detectable based on group-averaging in a larger population. Accordingly, in Experiment 4 we scanned thirty-one individuals (other than those who participated in Experiments 1-3) while they were presented with the same stimuli as in Experiment 1 (Figure 6A).

As demonstrated in Figure 3B, PIGS was also detectable in this new population in almost the same location as in Experiment 1. Specifically, PIGS was detected bilaterally within the posterior portion of the intraparietal gyrus, adjacent to the POS. We did not find a significant difference between the two populations in the size of PIGS when normalized either relative to the size of RSC ($t(43)=0.98$, $p=0.33$), TOS ($t(43)=0.26$, $p=0.80$) or PPA ($t(43)=0.52$, $p=0.61$). Thus, the location and relative size of PIGS appeared to remain unchanged across populations.

These results suggest that one may rely on the probabilistically-generated labels to examine the evoked activity within PIGS. To test this hypothesis, we measured the level of scene-selective activity in PIGS, along with the areas TOS, RSC and V6, using the probabilistic labels generated based on the results of Experiments 1 and 3 (see Methods and Figure 5). As demonstrated in Figure 6B-C, results of this ROI analysis showed a significant scene-selective activity in PIGS ($t(31)=8.11$, $p<10^{-8}$), TOS ($t(31)=7.91$, $p<10^{-7}$) and RSC ($t(31)=9.11$, $p<10^{-8}$). More importantly, despite the proximity of PIGS and V6, the level of scene-selective activity in PIGS was significantly higher than V6 ($t(11)=5.03$, $p<10^{-4}$). Thus, it appears that the probabilistically-generated ROIs could be used to examine PIGS response, and to differentiate it from the adjacent areas such as V6 (see also Experiment 5).

3.4. Experiments 5 – Selective response to scenes compared to non-scene objects in PIGS

So far, we have localized PIGs in multiple experiments by contrasting the response evoked by scenes vs. faces. In Experiment 5, we examined whether PIGS also showed a selective response to scenes compared to (non-face) objects. Twelve individuals, other than those who participated in Experiments 1-3, participated in this experiment. Subjects were presented with pictures of scenes (other than those used to localize PIGS) and everyday objects (Figure 6D).

As in Experiment 4, we used the probabilistically-generated labels based on the results of Experiments 1 and 3. Here again (Figure 6E-F), we found significant scene-selective activity within PIGS ($t(11)=6.57$, $p<10^{-4}$), RSC ($t(12)=11.00$, $p<10^{-6}$) and TOS ($t(12)=6.26$, $p<10^{-3}$). We also found that the level of scene-selective activity within PIGS is significantly stronger than the adjacent area V6 ($t(11)=2.42$, $p=0.03$). Thus, scenes and (non-face) objects are differentiable from each other based on the activity evoked within PIGS.

3.5. Experiment 6 – PIGS response to ego-motion

Experiments 1-5 clarified PIGS location and selectivity for scenes. But the specific role of this area in scene perception remains unknown. Experiment 5 tests the hypothesis that area PIGS is involved in encoding ego-motion within scenes. This hypothesis was motivated by the fact that PIGS is located adjacent to V6 (Figure 5D), an area involved in encoding optic-flow. Other studies had also suggested an interaction between ego-motion and scene signals within this region, without clarifying whether this activity was centered either within or outside V6 (Pitzalis *et al.*, 2020; Sulpizio *et al.*, 2020).

Twelve individuals, from those who participated in Experiment 1, took part in this experiment (see Methods). They were presented with coherently changing scene stimuli that implied ego-motion across different outdoor trails (Figure 7). On separate blocks, they were also presented with incoherently changing scenes and faces. Figure 8 shows the group-average scene-selective activity, evoked by coherently (Figure 8A) and incoherently changing scene stimuli (Figure 8B). Consistent with our hypothesis, PIGS showed a significantly stronger response (bilaterally) to coherently (compared to incoherently) changing scenes that implied ego-motion (Figure 8C). But the level of activity within RSC and TOS did not change significantly between these two conditions.

Consistent with the group-averaged activity maps, results of an ROI analysis (Figure 9) yielded a significantly stronger response to coherently (vs. incoherently) changing scenes in PIGS ($t(11)=5.97$, $p<10^{-4}$) but not in RSC ($t(11)=0.12$, $p=0.90$) and TOS ($t(11)=0.48$, $p=0.64$). Interestingly, area PPA showed a stronger response to incoherently compared to coherently changing scenes ($t(11)=3.48$, $p<0.01$). To better highlight the difference between scene-selective areas, we repeated this test by applying a one-way repeated measures ANOVA to the differential response to “coherently - incoherently changing scenes”, measured across these four scene-selective areas. This test yielded a significant effect of area on the evoked differential activity ($F(3, 11)=53.89$, $p<10^{-10}$). These results suggest a distinctive role for area

PIGS in ego-motion encoding that differentiates it from the other scene-selective areas. The absence of activity modulation in the other scene-selective areas also ruled out the possibility that the activity increase in PIGS was simply due to attentional modulation during coherently vs. incoherently changing scenes (see Discussion).

Besides PIGS, we also found a significantly stronger response to coherently rather than incoherently changing scenes in area V6 ($t(11)=3.57$, $p<0.01$). But the level of this selectivity was significantly weaker than PIGS ($t(11)=2.63$, $p=0.02$). Notably, in the group-averaged activity maps, the contrast between coherently vs. incoherently changing scenes also yielded a stronger response outside (rather than inside) the POS. Together, these results suggested that the center of interaction between the effects of scene vs. ego-motion presentation was within PIGS and not V6.

Finally, we also tested motion-selectivity of the PIGS response. Results of an ROI analysis, applied to the activity evoked by moving vs. stationary rings (see Methods), did not yield any significant motion-selective activity within PIGS ($t(11)=1.84$, $p=0.10$), RSC ($t(11)=1.97$, $p=0.08$), PPA ($t(11)=1.93$, $p=0.08$) and V6 ($t(11)=2.03$, $p=0.07$). In contrast, we found strong motion-selectivity within area TOS ($t(11)=4.57$, $p<10^{-3}$) most likely due to its overlap with the motion-selective area V3A/B (Nasr *et al.*, 2011). All in all, these results were consistent with previous studies of motion-selective response within scene-selective areas (Hacialihafiz and Bartels, 2015) and suggested that PIGS contribution to motion perception is limited to ego-motion in natural scenes.

4. Discussion

In this study, we challenged the overall idea that scene processing is limited to the function of PPA, RSC and TOS, and that the other smaller scene-selective sites are products of noise in fMRI measurements. By focusing on one small scene-selective site, located within the posterior intraparietal gyrus, we showed that this site (a.k.a. PIGS) was detectable consistently across individuals and groups. We also showed that inclusion of this site in the models of scene perception expands our understanding of how scene perception and ego-motion interact with each other.

4.1. FMRI and all that “noise, noise, noise”!

Like every other technique, the early fMRI studies dealt with a considerable amount of noise in measurements, partly due to using lower magnetic field scanners (e.g. 1.5T (Epstein and Kanwisher, 1998)) and imperfect hardware and software. This noise in measurements affected the reliability/reproducibility of the findings. Consequently, those early studies focused on larger activity sites that were more reliably detectable across subjects/sessions. The smaller sites were either ignored or eliminated by excessive signal smoothing, applied to enhance the level of contrast to noise ratio.

But, with advances in neuroimaging techniques (both software and hardware), today we can detect fine-scale activity sites in the spatial scale of cortical columns (Nasr *et al.*, 2016; Yacoub *et al.*, 2007; Zimmermann *et al.*, 2011) and layers (De Martino *et al.*, 2013; Finn *et al.*, 2021). Although the reliability of the fMRI signal still depends on the amount of trial repetitions, when repeated adequately, the evoked response can be detected reliably across different sessions, irrespective of the time gap between them (Kennedy *et al.*, 2022; Nasr *et al.*, 2016).

Directly related to our findings, here we have shown PIGS was located consistently across multiple subjects (Figures 1-3). We have also shown reproducibility of PIGS across sessions, one of them done in a 3T and the other one done in a 7T scanner (Figure 4). More importantly, our results indicated that the probabilistic labels, generated based on one population, can be used to localize PIGS and to distinguish its function from the adjacent regions (e.g. V6) in the second population (Figure 6). These results rule out the possibility that PIGS, despite its small size, is just a product of noise in the measurements.

4.2. PIGS responds selectively to a variety of scene stimuli

Selective response in one brain region could be simply due to the limited number of stimuli used to evoke the response. To show a true category-selective response, the stimulus set should include enough samples to represent the diversity among the category members. Accordingly, we used four different scene stimulus sets across our experiments that included a wide variety of indoor/outdoor and natural/manmade scenes. In all cases, we were able to evoke a selective response within PIGS area, and the level of this response, was comparable to the adjacent scene-selective areas RSC and TOS. Thus, PIGS scene-selective response appeared not to be limited to a subset of scenes. However, it remains unclear whether scene stimuli are differentiable from each other based on the pattern of evoked response in this region. More experiments in the future are necessary to test this hypothesis.

4.3. Not just another scene selective area

Our results (Experiment 6) suggest that ego-motion can largely influence the activity evoked within PIGS. This phenomenon distinguishes PIGS role in scene perception from the other scene-selective regions. Specifically, previous studies have shown that, among scene-selective areas, PPA and RSC show weak-to-no sensitivity to motion (Hacialihafiz and Bartels, 2015). In comparison, area TOS shows a stronger motion-selective response, most likely due to its (partial) overlap with area V3A/B (Nasr *et al.*, 2011). But here, we showed that the ego-motion related activity within PIGS is stronger than TOS.

This phenomenon is consistent with the fact that PIGS is located adjacent to area V6 (Figures 4 and 5), an area that contributes in encoding optic flow (Dechent and Frahm, 2003; Pitzalis *et al.*, 2009). In this condition, the likely inputs from V6 may contribute to the strong ego-motion selective response in PIGS. However, PIGS and V6 roles in ego-motion encoding are also different from each other. Specifically, compared to V6, PIGS showed a stronger sensitivity to the interaction between scene presentation and ego-motion (Figure 9). But V6 shows a stronger response to optic flow induced by random dots (Figures 4 and 5). Thus, PIGS contributes to encoding the interaction between scene perception and ego motion, while V6 is likely involved in detecting optic-flow caused by ego-motion.

4.4. Ego-motion but not attention

In Experiment 6, we showed stronger scene-selective activity within PIGS as subjects were presented with coherently (compared to incoherently) changing scenes. It could be argued that this phenomenon is due to attentional modulation. According to this hypothesis, coherently changing scenes attract more attention compared to incoherently changing scenes. Although at the first glance, this hypothesis appears to be consistent with the intraparietal role in controlling the spatial attention (Behrmann *et al.*, 2004; Colby and Goldberg, 1999; Szczepanski *et al.*, 2010), it appears inconsistent with the other studies of attention to scenes. Specifically, multiple studies have already shown that attention to scenes increases the level of activity within PPA and the other scene-selective areas (Baldauf and Desimone, 2014; Kanwisher and Wojciulik, 2000; Nasr and Tootell, 2012; O'craven *et al.*, 1999). But here, we did not find any activity increase in response to coherently (vs. incoherently) changing scenes in PPA, RSC and TOS. Thus, modulation of attention, per se, could not be responsible for PIGS sensitivity to the

interaction between the effects of scene and ego-motion.

4.5. Direction-selective response within the intraparietal cortex

Traditionally, motion-selective sites are expected to show at least some levels of sensitivity to motion direction. Evidence for this phenomenon has been shown previously in other visual areas in humans (Kennedy *et al.*, 2022; Zimmermann *et al.*, 2011) and NHPs (Albright *et al.*, 1984; Lu *et al.*, 2010). In this study, we did not test the sensitivity of PIGS response to the direction of ego motion. However, multiple studies have already shown evidence for sensitivity to motion direction across the interparietal region. For instance, Pitzalis et al. have shown evidence for motion direction encoding within V6+ region (Pitzalis *et al.*, 2020). Furthermore, a study by Tootell et al. has shown evidence for motion direction (looming vs. withdrawing) encoding within the intraparietal region (Tootell *et al.*, 2022). Although none of these studies showed any evidence for a new scene-selective area, they raised the possibility that PIGS may also contribute in encoding ego-motion direction and even higher level cognitive concepts such as detecting an intrusion to personal space (Holt *et al.*, 2014). More studies are necessary to test these possibilities directly.

4.6. Limitations

Previous studies have suggested that scene-selective areas are functionally connected to each other (Baldassano *et al.*, 2013; Li *et al.*, 2022; Nasr *et al.*, 2013). Although our findings suggest that PIGS is a part of the scene-selective network, the exact functional connection between PIGS and the other scene-selective areas remains unclear. Accordingly, more functional connectivity studies are required to clarify this point. These studies may also clarify the potential functional connection between PIGS and motion-selective areas such as V6, V3A and MT.

5. Conclusion

For more than two decades, neuroimaging studies of scene perception focused on linking scene perception to the evoked activity within PPA, TOS/OPA and RSC – three large scene-selective areas within the human visual cortex. Although other scene-selective sites can be easily detected across the visual cortex, they have been largely ignored due to their relatively small size. In this study we challenged this simplified model of scene perception by showing that there

are more scene-selective regions within the human visual cortex than we thought. Our findings highlighted the fact that inclusion of these small sites in models of scene perception is likely crucial for understanding scene processing in more dynamic environments.

Figure Captions

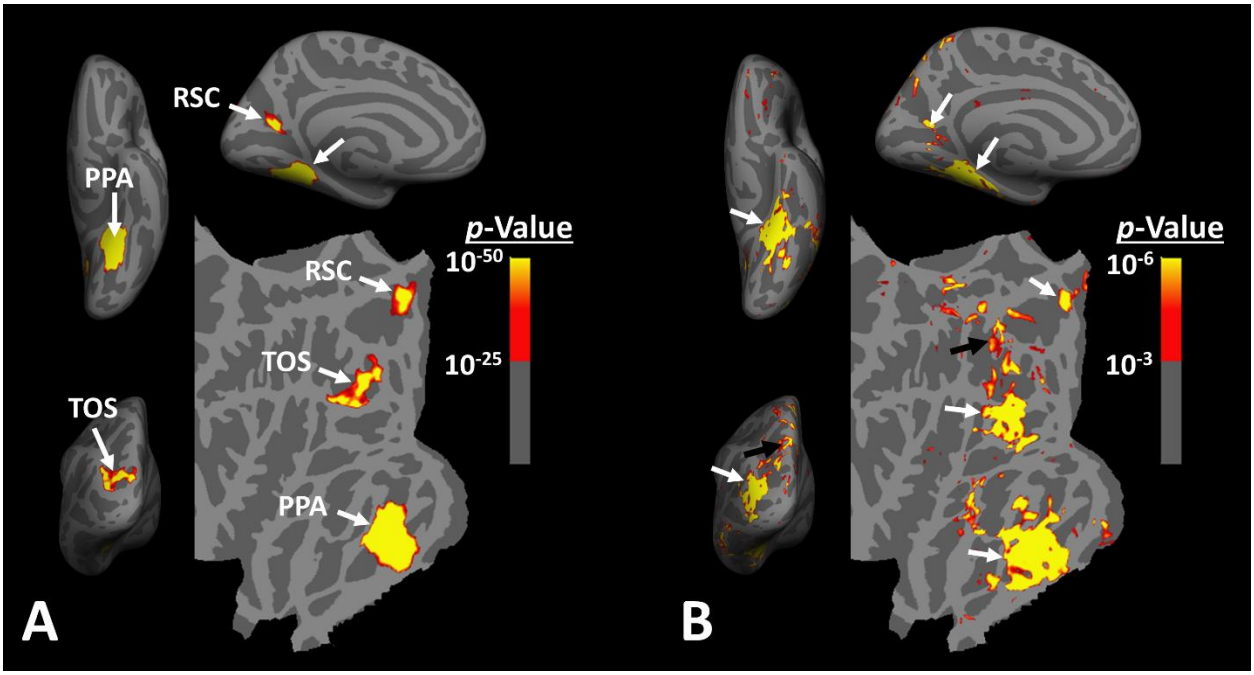

Figure 1) Distribution of scene-selective areas in human visual cortex. Panel **A** shows the group-averaged (n=14) response to "scenes > faces" contrast (Experiment 1). Areas PPA, RSC and TOS/OPA are localized within the temporal, medial and posterior-lateral brain surfaces, respectively. To show consistency with our previous reports (Nasr *et al.*, 2011), data from individual subjects was largely smoothed (FWHM=5mm) and the group-averaged maps were generated based on fixed- rather than random-effects (see also Figure 3). The resultant map was thresholded at $p<10^{-25}$ and overlaid on the common brain template (fsaverage). Panel **B** shows the activity map in one randomly-selected subject (see also Figure 2), evoked in response to the same stimulus contrast as in Panel **A**. Here, the activity map was only minimally smoothed (FWHM=2mm). Consequently, multiple smaller scene-selective sites could be detected across the cortex, including PIGS (black arrowhead), located within the posterior intraparietal gyrus. Traditionally, these smaller activity patches are treated as noise in measurement and discarded. For ease in comparing the two panels, the individual's data was also overlaid on fsaverage.

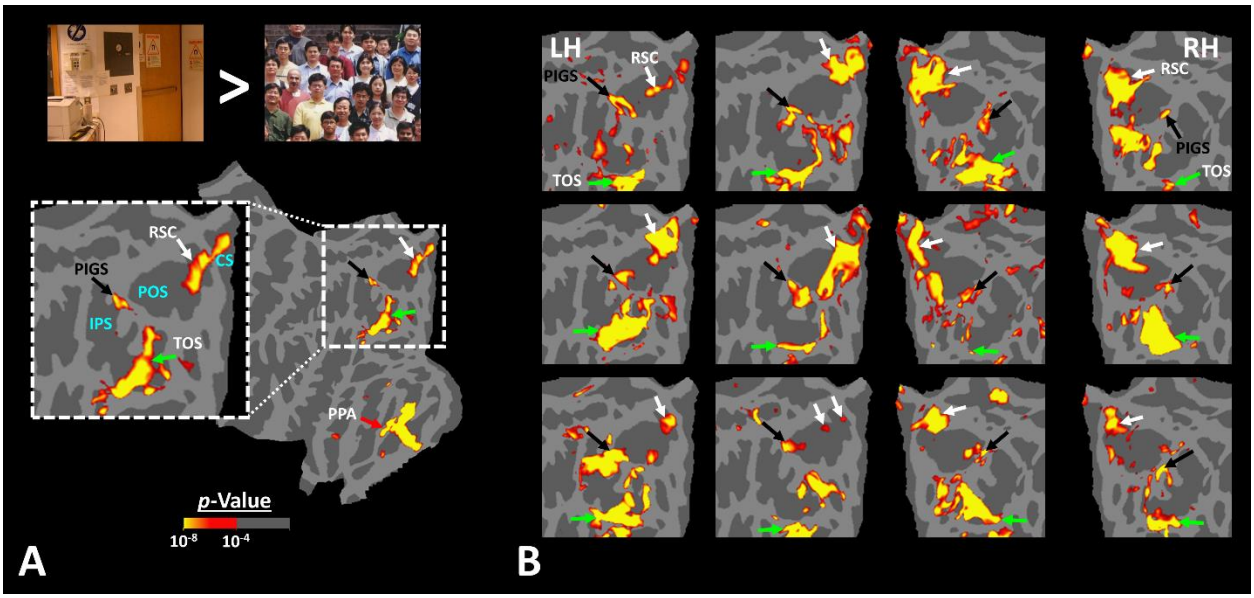

Figure 2) Activity evoked by 'scene>face' contrast in seven individual subjects, other the one shown in Figure 1. Panel **A** shows the evoked activity in the right hemisphere of one individual subject. The inset shows the enlarged activity map within the intraparietal region. The three scene-selective areas, along with area PIGS are indicated in the map with arrowheads. The location of adjacent sulci (POS), the intraparietal sulcus (IPS) and the calcarine sulcus (CS)) are also indicated in the inset. Panel **B** shows the result from six other individuals. In this panel, the first two columns show the activity within the left hemisphere, while the next two columns show the activity within the right hemisphere of the same subjects. In all subjects, PIGS is detectable bilaterally within the posterior portion of the intraparietal gyrus, near (outside) the POS. All activity maps were overlaid on the fsaverage to highlight the consistency in PIGS location across subjects.

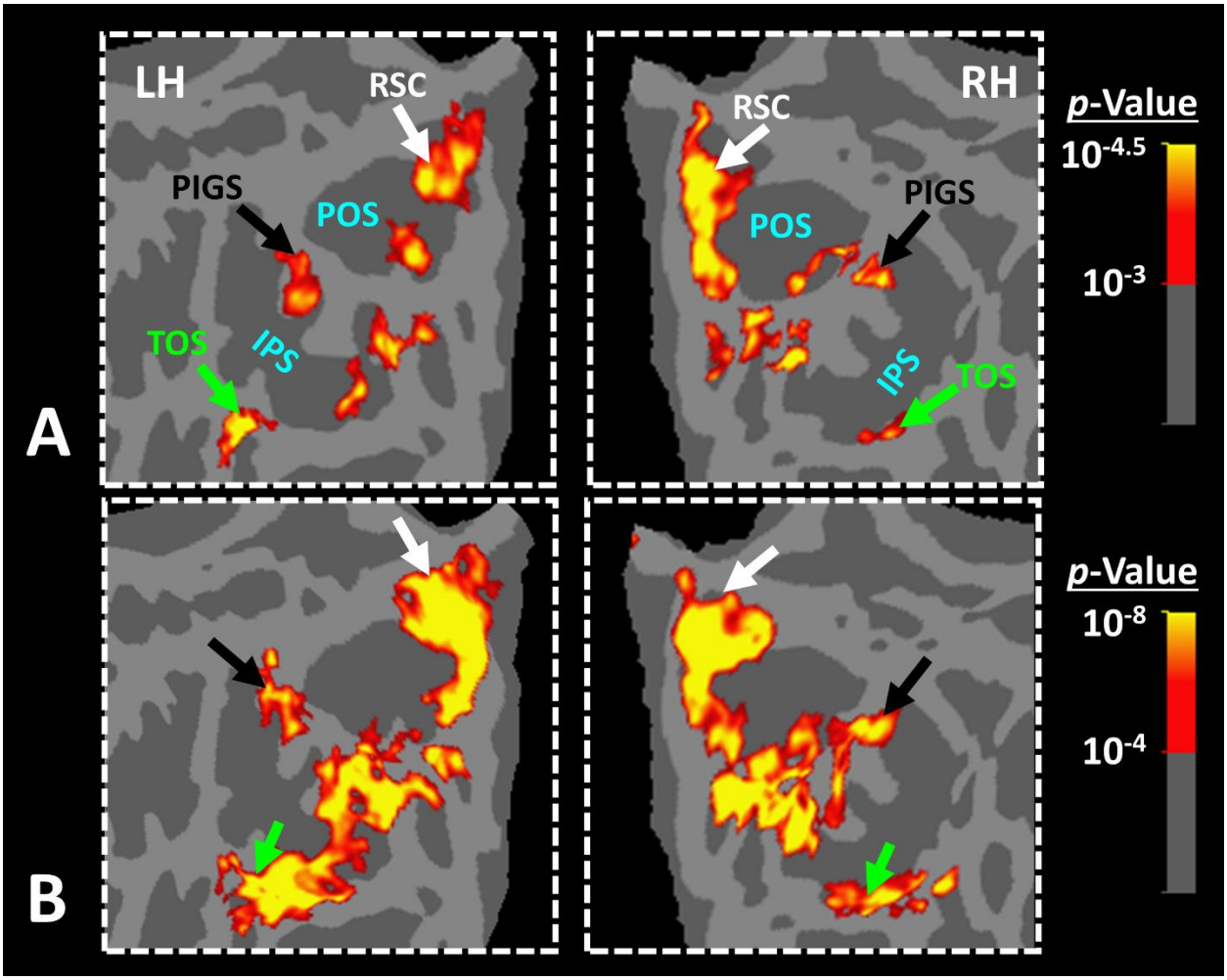

Figure 3) PIGS was detected in group-averaged activity maps across two non-overlapping populations. Panel **A** shows the grouped-average activity, evoked within the intraparietal region of fourteen subjects who participated in Experiment 1. Panel **B** shows the grouped-average activity, evoked within the intraparietal region of thirty-one subjects who participated in Experiment 4. Importantly, area PIGS was detectable in both panels bilaterally in the same location. Thus, despite its small size, this area was detectable even in the group-averaged maps based on large populations. Notably, in both panels, maps were generated based on random-effects, after correction for multiple comparisons. In both maps, location of PIGS, RSC and TOS are indicated with arrowheads.

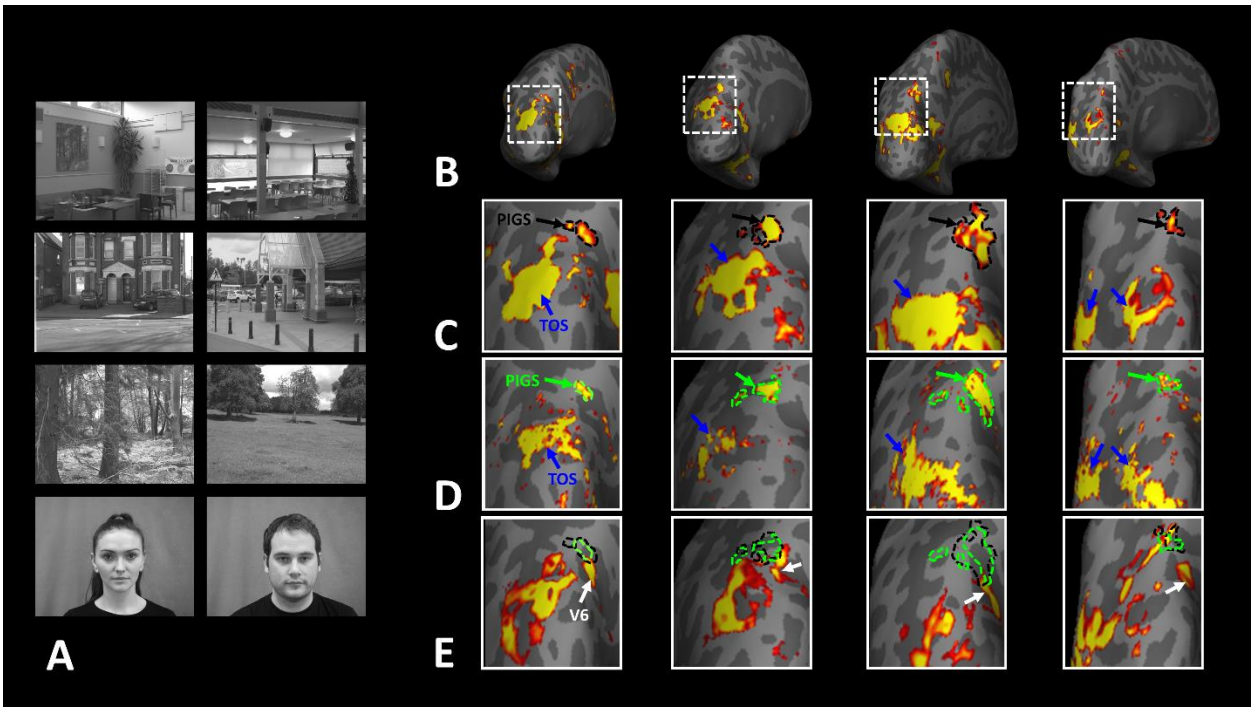

Figure 4) PIGS was detectable consistently across sessions. Panel **A** shows the stimuli used for localizing PIGS during 7T scans. Stimuli including indoor, manmade outdoor and natural outdoor scenes and faces other than those used in Experiment 1. Panels **B and C** show the evoked activity by 'scene>face' contrast in the 3T scans (Experiment 1), overlaid on subjects own reconstructed brain (left hemisphere). Panel **D** shows the evoked activity by 'scene>face' contrast during 7T scans (Experiment 2). Despite the change in the scanner (3T vs. 7T) and stimuli, PIGS location remains mostly unchanged. Panel **E** shows the location of PIGS, measured in 3T/7T (black/green dashed lines) relative to the location of area V6 (white arrowhead), localized functionally based on the response to optic-flow>random motion (Experiment 3). In all subjects, the center of scene- and optic-flow-selective responses appear to be adjacent, but not overlapping.

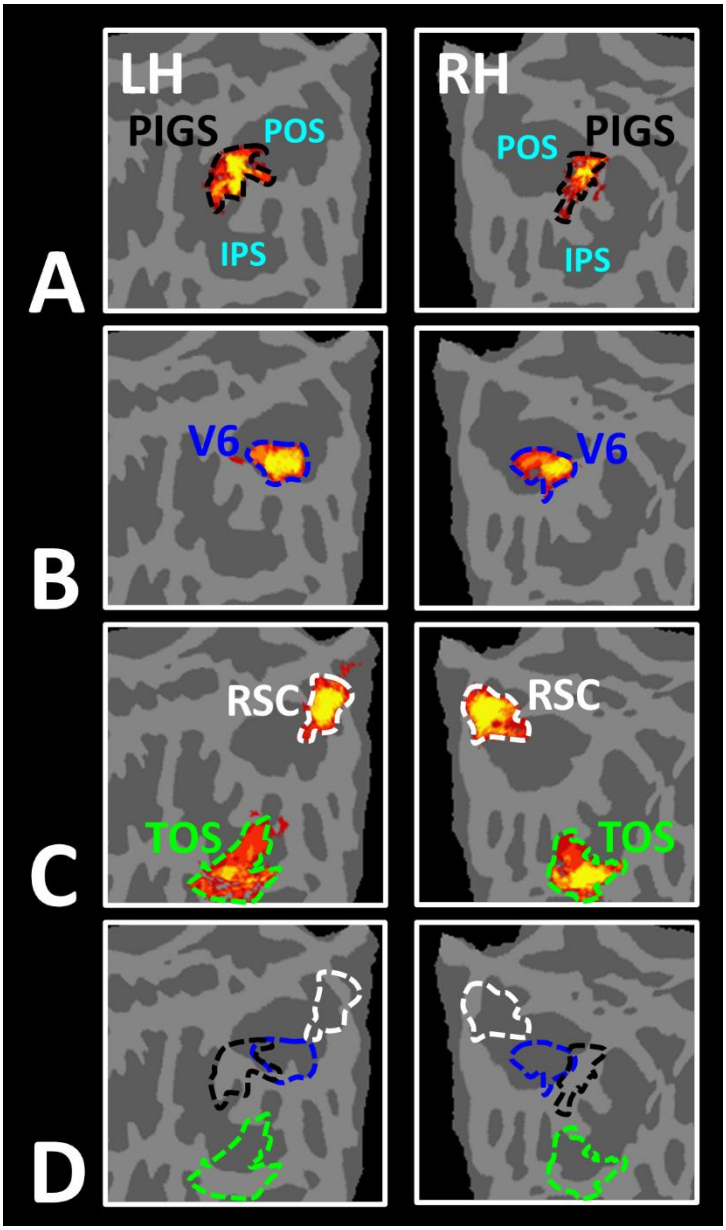

585

586 **Figure 5)** Area PIGS is located outside the POS and adjacent to the functionally-localized area
587 V6. Panels **A-C** show the probabilistic localization of areas PIGS, V6, RSC and TOS,
588 respectively (see Methods). All probability maps are thresholded at 20%-50% (red-to-yellow)
589 and overlaid on fsaverage. Panel **D** shows the relative location of these sites. Consistent with
590 the results from the individual maps (Figure 4E), PIGS and V6 were located adjacent to each
591 other, with V6 located within the POS and PIGS located outside the POS (within the intraparietal
592 gyrus).

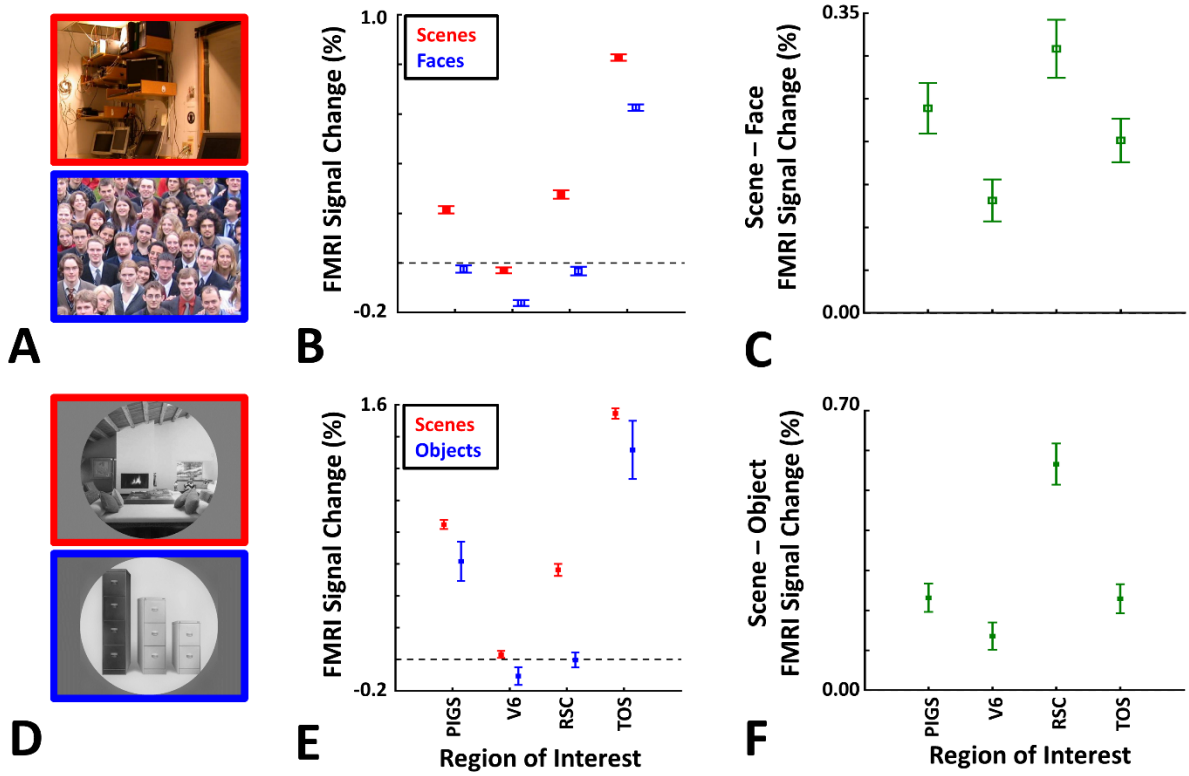

Figure 6) Probabilistically generated labels can be used to detect PIGS. Panels **A and D** show the example of stimuli used in Experiments 4 and 5, respectively. Panels **B and E** show the activity evoked by 'scenes vs. faces' and 'scenes vs. objects' stimuli, across PIGS, V6, RSC and TOS. Panels **C and F** show the level of scene-selective activity within these regions. Despite the small size of PIGS, in both experiments, the probabilistic label could detect scene-selective activity within this area and the level of this activity was significantly higher than the adjacent area V6. In all panels, error bars represented one standard error of mean.

Figure 7) Example of stimuli used in Experiment 6. Coherently changing scenes implied ego-motion as if the observer was jogging through a trail. Incoherently changing scenes consisted of the same scene images as the coherently changing scenes, presented in a random order. Face stimuli consisted of a mosaic of faces. These stimuli were different than those used in the previous experiments.

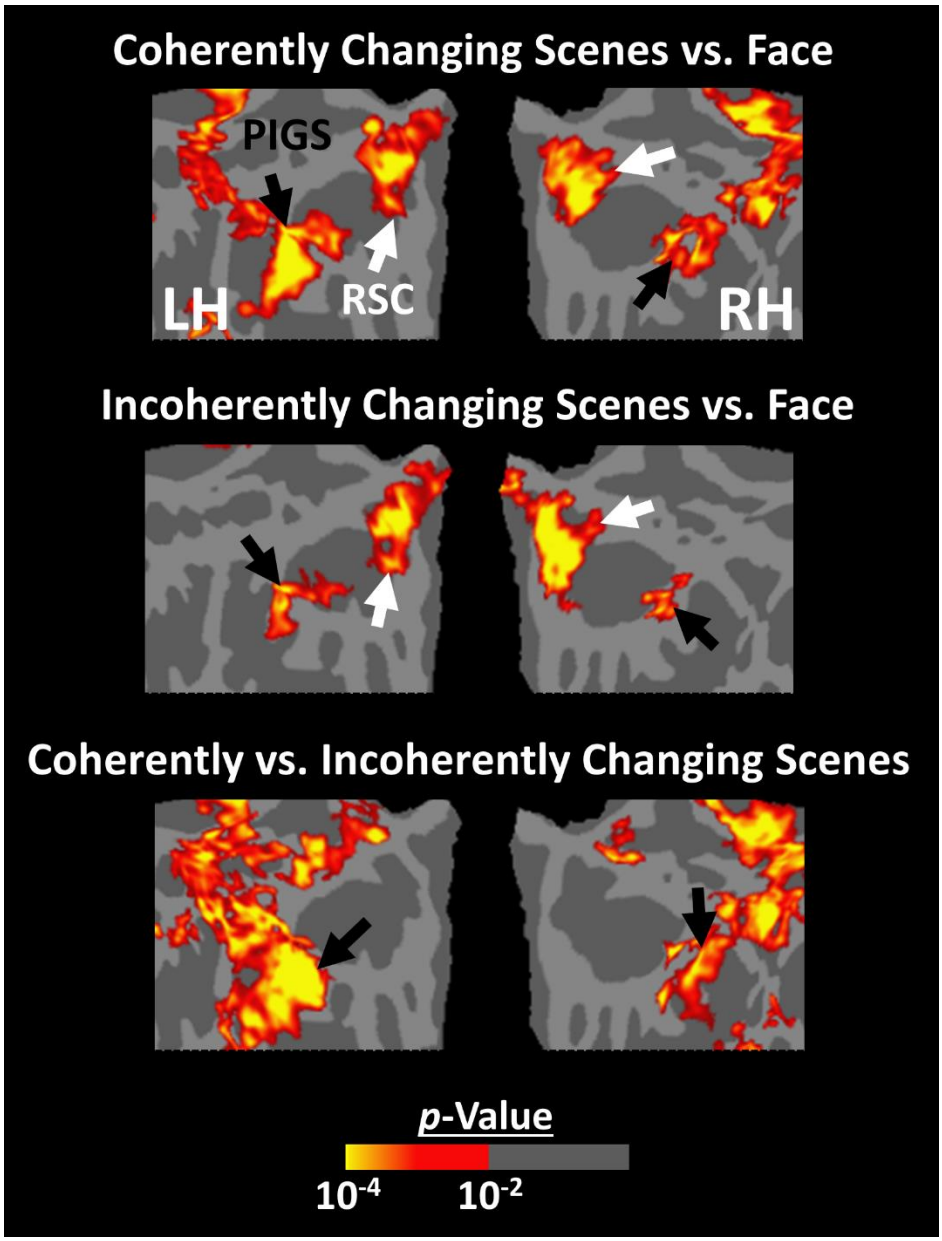

Figure 8) Scene-selective response to coherently vs. incoherently changing scenes within the intraparietal region (Experiment 6). The first two rows show the group-averaged activity evoked by coherently (top) and incoherently (middle) changing scenes relative to faces. The bottom panel show the group-averaged response evoked by the 'coherently > incoherently moving scenes' contrast. Among scene-selective areas, only PIGS showed significant sensitivity to the observer ego-motion. All maps were generated based on random-effects after correction for multiple comparisons. The location of PIGS (outside the POS) and RSC (within the POS) are indicated by black and white arrowheads, respectively.

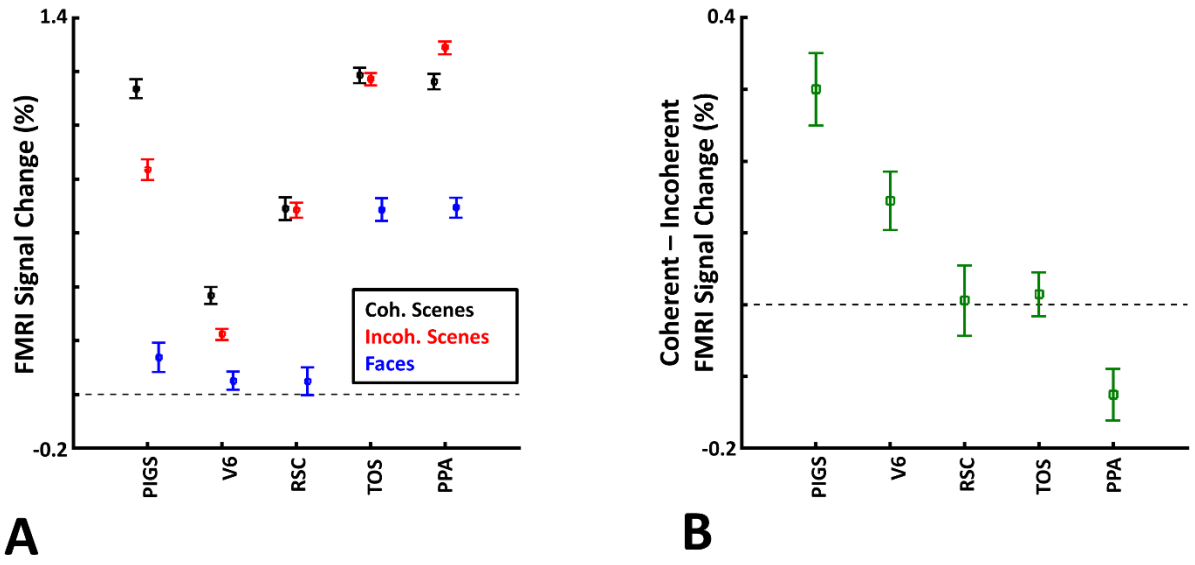

Figure 9) The activity evoked within PIGS is sensitive to the interaction between scene presentation and the observer ego-motion. Panel **A** shows the activity evoked by the coherently (black) and incoherently moving scenes (red) along with the faces (blue), across areas PIGS, V6, RSC, TOS and PPA. Panel **B** shows the level of difference between the response evoked by 'coherently – incoherently' moving scenes across the regions of interest. While all regions showed a significantly stronger response to scenes compared to faces, PIGS showed the strongest sensitivity to the interaction between scene and ego-motion signals. Notably, compared to PIGS, area V6 showed a stronger sensitivity to optic-flow generated based on random dots (Experiment 3). Error bars represented one standard error of mean.

References

Adams, W.J., Elder, J.H., Graf, E.W., Leyland, J., Lugtigheid, A.J., Muryy, A., 2016. The southampton-york natural scenes (syns) dataset: Statistics of surface attitude. *Sci. Rep.* 6**,** 1-17.

Albright, T.D., Desimone, R., Gross, C.G., 1984. Columnar organization of directionally selective cells in visual area MT of the macaque. *J. Neurophysiol.* 51**,** 16-31.

Baldassano, C., Beck, D.M., Fei-Fei, L., 2013. Differential connectivity within the Parahippocampal Place Area. *Neuroimage* 75**,** 228-237.

Baldauf, D., Desimone, R., 2014. Neural mechanisms of object-based attention. *Science* 344**,** 424-427.

Behrmann, M., Geng, J.J., Shomstein, S., 2004. Parietal cortex and attention. *Curr. Opin. Neurobiol.* 14**,** 212-217.

Brainard, D.H., 1997. The Psychophysics Toolbox. *Spat. Vis.* 10**,** 433-436.

Colby, C.L., Goldberg, M.E., 1999. Space and attention in parietal cortex. *Annu. Rev. Neurosci.* 22**,** 319-349.

Dale, A.M., Fischl, B., Sereno, M.I., 1999. Cortical surface-based analysis. I. Segmentation and surface reconstruction. *Neuroimage* 9**,** 179-194.

De Martino, F., Zimmermann, J., Muckli, L., Ugurbil, K., Yacoub, E., Goebel, R., 2013. Cortical depth dependent functional responses in humans at 7T: improved specificity with 3D GRASE. *PLoS One* 8**,** e60514.

Dechent, P., Frahm, J., 2003. Characterization of the human visual V6 complex by functional magnetic resonance imaging. *Eur. J. Neurosci.* 17**,** 2201-2211.

Dilks, D.D., Julian, J.B., Paunov, A.M., Kanwisher, N., 2013. The occipital place area is causally and selectively involved in scene perception. *J. Neurosci.* 33**,** 1331-1336.

Epstein, R., Kanwisher, N., 1998. A cortical representation of the local visual environment. *Nature* 392**,** 598-601.

Finn, E.S., Huber, L., Bandettini, P.A., 2021. Higher and deeper: Bringing layer fMRI to association cortex. *Prog. Neurobiol.* 207**,** 101930.

Fischl, B., 2012. FreeSurfer. *Neuroimage* 62**,** 774-781.

Fischl, B., Salat, D.H., Busa, E., Albert, M., Dieterich, M., Haselgrove, C., van der Kouwe, A., Killiany, R., Kennedy, D., Klaveness, S., Montillo, A., Makris, N., Rosen, B., Dale, A.M., 2002. Whole brain segmentation: automated labeling of neuroanatomical structures in the human brain. *Neuron* 33**,** 341-355.

Fischl, B., Sereno, M.I., Dale, A.M., 1999. Cortical surface-based analysis. II: Inflation, flattening, and a surface-based coordinate system. *Neuroimage* 9**,** 195-207.

Friston, K.J., Holmes, A.P., Price, C.J., Buchel, C., Worsley, K.J., 1999. Multisubject fMRI studies and conjunction analyses. *Neuroimage* 10**,** 385-396.

Greve, D.N., Fischl, B., 2009. Accurate and robust brain image alignment using boundary-based registration. *Neuroimage* 48**,** 63-72.

Grill-Spector, K., 2003. The neural basis of object perception. *Curr. Opin. Neurobiol.* 13**,** 159-166.

Hacialihafiz, D.K., Bartels, A., 2015. Motion responses in scene-selective regions. *Neuroimage* 118**,** 438-444.

Holt, D.J., Cassidy, B.S., Yue, X., Rauch, S.L., Boeke, E.A., Nasr, S., Tootell, R.B., Coombs, G., 3rd, 2014. Neural correlates of personal space intrusion. *J. Neurosci.* 34**,** 4123-4134.

Kanwisher, N., Wojciulik, E., 2000. Visual attention: insights from brain imaging. *Nature reviews neuroscience* 1**,** 91-100.

Kennedy, B., Bex, P., Hunter, D., Nasr, S., 2022. Two fine-scale channels for encoding motion and stereopsis within the human magnocellular stream. *Prog. Neurobiol.***,** 102374.

Koopmans, P.J., Barth, M., Norris, D.G., 2010. Layer-specific BOLD activation in human V1. *Hum. Brain Mapp.* 31**,** 1297-1304.

Levy, I., Hasson, U., Harel, M., Malach, R., 2004. Functional analysis of the periphery effect in human building related areas. *Hum. Brain Mapp.* 22**,** 15-26.

Li, X., Zhu, Q., Vanduffel, W., 2022. Submillimeter fMRI reveals an extensive, fine-grained and functionally-relevant scene-processing network in monkeys. *Prog. Neurobiol.* 211**,** 102230.

Lu, H.D., Chen, G., Tanigawa, H., Roe, A.W., 2010. A motion direction map in macaque V2. *Neuron* 68**,** 1002-1013.

Maguire, E., 2001. The retrosplenial contribution to human navigation: a review of lesion and neuroimaging findings. *Scand. J. Psychol.* 42**,** 225-238.

Nasr, S., Devaney, K.J., Tootell, R.B., 2013. Spatial encoding and underlying circuitry in scene-selective cortex. *Neuroimage* 83**,** 892-900.

Nasr, S., Liu, N., Devaney, K.J., Yue, X., Rajimehr, R., Ungerleider, L.G., Tootell, R.B., 2011. Scene-selective cortical regions in human and nonhuman primates. *J. Neurosci.* 31**,** 13771-13785.

Nasr, S., Polimeni, J.R., Tootell, R.B., 2016. Interdigitated Color- and Disparity-Selective Columns within Human Visual Cortical Areas V2 and V3. *J. Neurosci.* 36**,** 1841-1857.

Nasr, S., Tootell, R.B., 2012. Role of fusiform and anterior temporal cortical areas in facial recognition. *Neuroimage* 63**,** 1743-1753.

O'craven, K.M., Downing, P.E., Kanwisher, N., 1999. fMRI evidence for objects as the units of attentional selection. *Nature* 401**,** 584-587.

Park, S., Chun, M.M., 2009. Different roles of the parahippocampal place area (PPA) and retrosplenial cortex (RSC) in panoramic scene perception. *Neuroimage* 47**,** 1747-1756.

Pelli, D.G., 1997. The VideoToolbox software for visual psychophysics: transforming numbers into movies. *Spat. Vis.* 10**,** 437-442.

Pitzalis, S., Fattori, P., Galletti, C., 2015. The human cortical areas V6 and V6A. *Vis. Neurosci.* 32.

Pitzalis, S., Sereno, M.I., Committeri, G., Fattori, P., Galati, G., Patria, F., Galletti, C., 2009. Human V6: the medial motion area. *Cereb. Cortex* 20**,** 411-424.

Pitzalis, S., Serra, C., Sulpizio, V., Committeri, G., de Pasquale, F., Fattori, P., Galletti, C., Sepe, R., Galati, G., 2020. Neural bases of self-and object-motion in a naturalistic vision. *Hum. Brain Mapp.* 41**,** 1084-1111.

Polimeni, J.R., Bhat, H., Witzel, T., Benner, T., Feiweier, T., Inati, S.J., Renvall, V., Heberlein, K., Wald, L.L., 2015. Reducing sensitivity losses due to respiration and motion in accelerated echo planar imaging by reordering the autocalibration data acquisition. *Magn. Reson. Med.*

Polimeni, J.R., Fischl, B., Greve, D.N., Wald, L.L., 2010. Laminar analysis of 7T BOLD using an imposed spatial activation pattern in human V1. *Neuroimage* 52**,** 1334-1346.

Rajimehr, R., Young, J.C., Tootell, R.B., 2009. An anterior temporal face patch in human cortex, predicted by macaque maps. *Proc. Natl. Acad. Sci. U. S. A.* 106**,** 1995-2000.

Sulpizio, V., Galati, G., Fattori, P., Galletti, C., Pitzalis, S., 2020. A common neural substrate for processing scenes and egomotion-compatible visual motion. *Brain structure and Function* 225**,** 2091-2110.

Szczepanski, S.M., Konen, C.S., Kastner, S., 2010. Mechanisms of spatial attention control in frontal and parietal cortex. *J. Neurosci.* 30**,** 148-160.

Tootell, R.B., Nasiriavanaki, Z., Babadi, B., Greve, D.N., Nasr, S., Holt, D.J., 2022. Interdigitated Columnar Representation of Personal Space and Visual Space in Human Parietal Cortex. *J. Neurosci.* 42**,** 9011-9029.

Tsao, D.Y., Moeller, S., Freiwald, W.A., 2008. Comparing face patch systems in macaques and humans. *Proc. Natl. Acad. Sci. U. S. A.* 105**,** 19514-19519.

Yacoub, E., Shmuel, A., Logothetis, N., Ugurbil, K., 2007. Robust detection of ocular dominance columns in humans using Hahn Spin Echo BOLD functional MRI at 7 Tesla. *Neuroimage* 37**,** 1161-1177.

Zimmermann, J., Goebel, R., De Martino, F., van de Moortele, P.F., Feinberg, D., Adriany, G., Chaimow, D., Shmuel, A., Ugurbil, K., Yacoub, E., 2011. Mapping the organization of axis of motion selective features in human area MT using high-field fMRI. *PLoS One* 6**,** e28716.